HHS Public Access

Author manuscript

Neuropharmacology. Author manuscript; available in PMC 2020 November 01.

Published in final edited form as:

Neuropharmacology. 2019 November 01; 158: 107597. doi:10.1016/j.neuropharm.2019.04.003.

The Highly Selective Dopamine D_3R Antagonist, *R*-VK4-40, Attenuates Oxycodone Reward and Augments Analgesia in Rodents

Chloe J. Jordan[1], **Bree Humburg**[1], **Myra Rice**[1], **Guo-Hua Bi**[1], **Zhi-Bing You**[1], **Anver Basha Shaik**[1], **Jianjing Cao**[1], **Alessandro Bonifazi**[1], **Alexandra Gadiano**[1,2,3], **Rana Rais**[2,3], **Barbara Slusher**[2,3], **Amy Hauck Newman**[1,*], **Zheng-Xiong Xi**[1,*]

[1]Molecular Targets and Medications Discovery Branch, National Institute on Drug Abuse, Intramural Research Program, Baltimore, MD 21224

[2]Johns Hopkins Drug Discovery, The Johns Hopkins University School of Medicine, 855 N. Wolfe Street, Baltimore, MD 21205

[3]Department of Neurology, The Johns Hopkins University School of Medicine, 855 N. Wolfe Street, Baltimore, MD 21205

Abstract

Prescription opioid abuse is a global crisis. New treatment strategies for pain and opioid use disorders are urgently required. We evaluated the effects of *R*-VK4-40, a highly selective dopamine (DA) D_3 receptor (D_3R) antagonist, on the rewarding and analgesic effects of oxycodone, the most commonly abused prescription opioid, in rats and mice. Systemic administration of *R*-VK4-40 dose-dependently inhibited oxycodone self-administration and shifted oxycodone dose-response curves downward in rats. Pretreatment with *R*-VK4-40 also dose-dependently lowered break-points for oxycodone under a progressive-ratio schedule. To determine whether a DA-dependent mechanism underlies the impact of D_3 antagonism in reducing opioid reward, we used optogenetic approaches to examine intracranial self-stimulation (ICSS) maintained by optical activation of ventral tegmental area (VTA) DA neurons in DAT-Cre mice. Photoactivation of VTA DA in non-drug treated mice produced robust ICSS behavior. Lower doses of oxycodone enhanced, while higher doses inhibited, optical ICSS. Pretreatment with *R*-VK4-40 blocked oxycodone-enhanced brain-stimulation reward. By itself, *R*-VK4-40 produced a modest dose-dependent reduction in optical ICSS. Pretreatment with *R*-VK4-40 did not compromise the antinociceptive effects of oxycodone in rats, and *R*-VK4-40 alone produced mild antinociceptive effects without altering open-field locomotion or rotarod locomotor performance. Together, these

[*]Corresponding authors: Amy Hauck Newman: 333 Cassell Dr., Baltimore, MD 21224, USA, Phone: (443)740-2887 amy.newman@nih.gov and Zheng-Xiong Xi: 251 Bayview Blvd, Baltimore, MD 21224, USA, Phone: (443)740-2517 ; zxi@mail.nih.gov.

Author Contributions: C.J., Z.-X. X., A.H.N. designed the experiments. C.J., B.H., M.*R*., Z.-B. Y., G.-H. B. performed the behavioral experiments. A.B.S. synthesized *R*-VK4-40. A.B. performed the binding assays. A.G., R.R., and B.S. conducted pharmacokinetics and metabolism assays and corresponding data analyses. C.J., B.H. and Z.-X. X. analyzed the data and prepared the figures. C.J., Z.-X. X. and A.H.N. wrote the manuscript.

findings suggest *R*-VK4-40 may permit a lower dose of prescription opioids for pain management, potentially mitigating tolerance and dependence, while diminishing reward potency. Hence, development of *R*-VK4-40 as a therapy for the treatment of opioid use disorders and/or pain is currently underway.

Keywords

Oxycodone; *R*-VK4-40; D_3 receptor antagonist; self-administration; brain-stimulation reward; opioid analgesia

INTRODUCTION

Prescription opioid abuse and overdose has become a crisis in the USA (Compton et al., 2016; Kenan et al., 2012; Meyer et al., 2014). Over 10 million Americans are estimated to have used prescription opioids nonmedically in 2016 (Compton et al., 2016; Jones et al., 2018). More than 70,000 Americans suffered fatal drug overdoses in 2017, an increase of more than 10% from the previous year, according to data from the Center for Disease Control and Prevention (CDC) (https://www.cdc.gov/nchs/nvss/vsrr/drug-overdose-data.htm). Although the United States Food and Drug Administration (FDA) has approved methadone and buprenorphine for the treatment of opioid abuse and addiction, there is a high rate of relapse after cessation of treatment. Further concerns for these opioid agonist therapies include their addictive liability, respiratory depression and withdrawal symptoms after cessation of use (Novick et al., 2015). Therefore, developing non-opioid medications for treatment of opioid abuse is essential.

Compelling preclinical evidence suggests that dopamine D_3 receptors (D_3R) may be a promising target in treatment of substance use disorders, particularly involving psychostimulants such as cocaine and methamphetamine (Heidbreder and Newman, 2010; Sokoloff and Le Foll, 2017). In rodents, blockade of D_3R with selective D_3R antagonists is highly effective in reducing relapse to drug-seeking behavior (Andreoli et al., 2003; Galaj et al., 2015; Gilbert et al., 2005; Higley et al., 2011; Vorel et al., 2002; Xi and Gardner, 2007; Xi et al., 2004). However, the efficacy of D_3R antagonists in modulation of psychostimulant self-administration remains controversial. Although evidence exists suggesting that D_3R blockade weakens conditioned place preference (CPP) to drugs of abuse (Ashby et al., 2003; Aujla and Beninger, 2005; Micheli et al., 2007; Song et al., 2013; Vorel et al., 2002) and inhibits electrical brain stimulation reward potentiated by these drugs (Higley et al., 2011; Pak et al., 2006; Spiller et al., 2008; Xi et al., 2006), other studies indicate that pharmacological blockade of D_3R has no effect on cocaine or methamphetamine self-administration maintained under low fixed-ratio (FR1, FR2) reinforcement schedules (Higley et al., 2011; Ross et al., 2007; Vorel et al., 2002; Xi et al., 2005).

In contrast to psychostimulants, we recently reported that D_3R antagonists appear to be more effective in reducing opioid reward during ongoing drug use. Pretreatment with BAK4-54 and CAB2-015, two D_3R antagonists/partial agonists with improved metabolic stability over previously investigated D_3R antagonists (Boateng et al., 2015; Keck et al., 2015), significantly inhibited intravenous heroin self-administration under FR1 reinforcement in

wild-type mice, but not in D_3-knockout mice (Boateng et al., 2015). In addition, BAK4-54, CAB2-015 and (±)VK4-116, a highly selective D_3R antagonist, dose-dependently inhibited oxycodone self-administration under FR1 and progressive-ratio (PR) reinforcement schedules and suppressed oxycodone-triggered reinstatement of drug-seeking behavior in rats (You et al., 2017). In the present study, we explored the utility of another novel D_3R antagonist, *R*-VK4-40, in the treatment of opioid abuse and addiction. (±)VK4-40 was recently reported as a highly D_3R selective partial agonist (compound 40 in Kumar et al., 2016). The *R*- and S-enantiomers were recently prepared and *R*-VK4-40 was determined to be a high affinity and highly selective D_3R antagonist (Figure 1). Given that previous studies have consistently demonstrated that blockade of D_3R attenuates reinstatement of drug-seeking behavior triggered by addictive drugs (Andreoli et al., 2003; Vorel et al., 2002; Xi and Gardner, 2007; You et al., 2017), stress (Xi et al., 2004) or drug associated cues (Aujla and Beninger, 2005; Galaj et al., 2015; Gilbert et al., 2005; Higley et al., 2011), in the present study we focused on the effects of *R*-VK4-40 on the reinforcing value of opioids. We first investigated the impact of *R*-VK4-40 on oxycodone self-administration under FR1 and PR reinforcement in rats. We then explored the capacity of *R*-VK4-40 to attenuate oxycodone-enhanced brain-stimulation reward maintained by optogenetic activation of midbrain DA neurons in DAT-cre mice. Lastly, because oxycodone is prescribed primarily to treat moderate to severe pain, we investigated the effects of *R*-VK4-40 on oxycodone analgesia to confirm that *R*-VK4-40 pretreatment does not compromise the therapeutic utility of opioids.

MATERIALS AND METHODS

Animals:

Male Long-Evans rats (275-325 g; Charles-River Laboratories, Raleigh, N.C.) were used throughout this study. Male heterozygous DAT-$Cre^{+/-}$ (DAT-Cre) mice were bred at the National Institute on Drug Abuse (NIDA) Intramural Research Program (IRP). All animals used in this study were housed in the animal facility at the NIDA IRP under a reversed 12 h light-dark cycle (lights on at 7:00 PM) with free access to food and water. All procedures were approved by the Animal Care and Use Committee (ACUC) of NIDA and were consistent with the *Guide for the Care and Use of Laboratory Animals, 8th edition* (National Research Council, 2011).

Experiment 1: R-VK4-40 binding assays

Membranes were prepared from HEK293 cells stably expressing human D_2 or D_3 receptors, grown in a 50:50 mix of DMEM and Ham's F12 culture media, supplemented with 20 mM HEPES, 2 mM L-glutamine, 0.1 mM non-essential amino acids, 1X antibiotic/antimycotic, 10% heat-inactivated fetal bovine serum, and 200 μg/ml hygromycin (Life Technologies, Grand Island, NY) and kept in an incubator at 37 °C and 5% CO_2. Cells were harvested using premixed Earle's Balanced Salt Solution (EBSS) with 5 mM EDTA (Life Technologies) and centrifuged at 3,000 rpm (~1,500 g) for 10 min at 21 °C. The supernatant was removed, and the pellet was re-suspended in 10 ml hypotonic lysis buffer (5 mM $MgCl_2$, 5 mM Tris, pH 7.4 at 4 °C) and centrifuged at 14,500 rpm (~25,000 g) for 30 min at 4 °C. The pellet was then resuspended in fresh EBSS buffer made from 8.7 g/L Earle's

Balanced Salts without phenol red (US Biological, Salem, MA), 2.2 g/L sodium bicarbonate, pH to 7.4. A Bradford protein assay (Bio-Rad, Hercules, CA) was used to determine the protein concentration and membranes were diluted to 500 μg/ml and stored at −80 °C for later use. Radioligand competition binding experiments were conducted using thawed membranes. Test compounds were dissolved in DMSO to a stock concentration of 10 mM and then diluted into 10 half-log serial dilutions using 30% DMSO vehicle. Previously frozen membranes were diluted in fresh EBSS to a 200 μg/ml (for D_2 or D_3). Radioligand competition experiments were conducted in 96-well plates containing 300 μl fresh EBSS buffer, 50 μl of diluted test compound, 100 μl of membranes (20 μg/well total protein for D_2 or D_3), and 50 μl of [^{3}H]*N*-methylspiperone (0.4 nM final concentration; Perkin Elmer). Nonspecific binding was determined using 10 μM (+)-butaclamol (Sigma-Aldrich, St. Louis, MO) and total binding was determined with 30% DMSO vehicle. All compound dilutions were tested in triplicate and the reaction incubated for one hour at room temperature. The reaction was terminated by filtration through a PerkinElmer Uni-Filter-96 GF/B, presoaked for 60 min in 0.5% polyethylenimine, using a Brandel 96-well plates Harvester manifold (Brandel Instruments, Gaithersburg, MD). The filters were washed 3 times with 3 ml (3 × 1 ml/well) of ice-cold binding buffer. Then 65 μL of PerkinElmer MicroScint 20 scintillation cocktail was added to each well, and filters were counted using a PerkinElmer MicroBeta microplate counter. IC_{50} values for each compound were determined from dose-response curves, and K_i values were calculated using the Cheng–Prusoff equation. K_d values for [^{3}H]*N*-methylspiperone were determined via separate homologous competitive binding experiments. K_i values were determined from at least three independent experiments and are reported as mean ± SEM.

Experiment 2: Metabolic stability of R-VK4-40 in rat liver microsomes

A phase I metabolic stability assay was conducted in rat liver microsomes purchased from BD Gentest (San Jose, CA, USA), as we have previously described (Kumar et al., 2016). The reaction was carried out with 100 mM potassium phosphate buffer, pH 7.4, in the presence of NADPH regenerating system (1.3 mM NADPH, 3.3 mM glucose 6-phosphate, 3.3 mM MgCl2, 0.4 U/mL glucose-6-phosphate dehydrogenase, 50 μM sodium citrate). Reactions in triplicate were initiated by addition of the liver microsomes to the incubation mixture (compound final concentration was 10 μM; 0.5 mg/mL microsomes). Compound disappearance was monitored via LC-MS/MS as described in bioanalysis below.

Experiment 3: Pharmacokinetic studies in rats

R-VK4-40 was administered peri-orally at a dose of 10 mg/kg in 25% β-hydroxy-cyclodextrin formulation. At pre-determined time points (0 min, 30 min, 60 min, 2 h, 4 h, and 8 h, n=3 rats per time point) animals were deeply anesthetized (100 mg/kg sodium pentobarbital, i.p.) and blood (~1 ml) was obtained via cardiac puncture and brain was dissected. Blood samples were centrifuged at 2,000 × g for 15 min, plasma was removed and all tissue was stored at −80 °C until LC-MS analysis.

For bioanalysis, standard curves were prepared in naïve plasma and brain tissues ranging from 0.01-50 nmol/mL. For extraction from plasma, standards and samples were thawed on ice, following which 25 μL of the calibration standard or sample were transferred into low

retention microcentrifuge tubes. 150 μL acetonitrile with internal standard (losartan) was added to each plasma sample for protein extraction. Brain samples were diluted 1:2 w/v with acetonitrile, and homogenized. Homogenized brain samples were vortex mixed and centrifuged at 10,000 g for 5 min; 25 μL of the supernatant was mixed with 100 μL of internal standard in acetonitrile for extraction. All samples were vortex mixed for 1 min and centrifuged at 10,000 gfor 10 min at 4°C. 50 μL of supernatant was transferred to a 250 μL polypropylene autosampler vials, mixed with 50μL water, and sealed with a Teflon cap. A volume of 3 μL was injected onto the ultraperformance liquid chromatography (UPLC) instrument for quantitative analysis using a temperature-controlled autosampler operating at 10°C.

Chromatographic analysis was performed using an Accela™ ultra high-performance system consisting of an analytical pump, and an autosampler coupled with TSQ Vantage mass spectrometer (Thermo Fisher Scientific Inc., Waltham MA). Separation of the analyte from potentially interfering material was achieved at ambient temperature using Agilent Eclipse Plus column (100 × 2.1mm i.d.) packed with a 1.8 μm C18 stationary phase. The mobile phase consisted of 0.1% formic acid in acetonitrile and 0.1% formic acid in H2O with gradient elution, starting with 10 % organic linearly increasing to 99 % and re-equilibrating to 10% until the end of the run. The total run time was 5.0 min. The selected reaction monitoring (SRM) transitions of *R*-VK4-40 and internal standard were m/z 454.827 to m/z 143.865 and m/z 423.03 to m/z 180.086, 207.086 respectively. Calibration curves for *R*-VK4-40 were computed using the peak area ratio of analyte to internal standard, with a quadratic regression curve fit and 1/x weighting factor. The equation generated from calibration curve was used to back-calculate concentrations of QC and unknown samples by interpolation method.

Experiment 4: Effects of R-VK4-40 on multiple-dose oxycodone self-administration tested under FR1 reinforcement

The intravenous (i.v.) catheterization surgery and i.v. oxycodone self-administration procedures were the same as reported previously (You et al., 2017). Briefly, a micro-renathane catheter was implanted in the right jugular vein under ketamine (90 mg/kg, i.p.) and xylazine (10 mg/kg, i.p.) anesthesia. The catheter was secured to the vein with suture silk and its free end was fed subcutaneously along the scapula to exit near the back of the skull. Next, the catheter was connected to a 22-gauge stainless connector that was mounted to the rat's skull using stainless steel screws and dental acrylic. After surgery, catheters were flushed with a gentamicin–heparin–saline solution (0.1 mg/ml gentamicin and 30 IU/ml heparin) to prevent clogging and infection. Animals recovered for at least 5 days before behavioral training started.

Oxycodone self-administration training was conducted in an operant conditioning chamber equipped with two response levers (Med Associates Inc., Georgia, VT, USA). Each rat was allowed daily in 3-h sessions to press the active lever for oxycodone infusions on a FR1 schedule of reinforcement. A response on the active lever resulted in the activation of light and tone cues and the infusion of an 0.08 ml oxycodone solution over 4.6 sec. This period also served as a timeout period during which the light and tone cues were kept on and the

animal's response on the active lever was recorded but had no scheduled consequence. Each animal's response on the inactive lever was recorded but had no consequences throughout testing.

Rats (n=8-11/group) were trained to self-administer oxycodone first at a higher dose (0.1 mg/kg/infusion) for 2 weeks, and then were switched to a lower dose (0.05 mg/kg/infusion) until stable self-administration was achieved, defined as 1) earning at least 20 oxycodone infusions or active lever responses under FR1 reinforcement during a 3-h session, 2) less than 20% variability in daily drug infusions across consecutive sessions, and 3) an active/inactive lever press ratio exceeding 2:1 (You et al., 2017; Zhan et al., 2018). The initial higher dose used for training was chosen based on our previous observation that 0.1 mg/kg/infusion produced the most rapid and facile acquisition of oxycodone self-administration. The subsequent lower dose of oxycodone was chosen in order to increase animals' work demand (i.e., lever presses) to achieve the same drug effect. In our experience, this approach increases sensitivity to detecting changes in drug-taking or drug-seeking behavior after pharmacological manipulation (Xi et al., 2006). After stable self-administration was achieved, the rats received either vehicle (25% 2-hydroxypropylβ-cyclodextrin) or one of two *R*-VK4-40 doses (10 or 20 mg/kg, i.p.), 30 min prior to the test session.

To determine whether *R*-VK4-40 alters oxycodone intake maintained by other doses of oxycodone, animals continued oxycodone self-administration of one of four other doses of oxycodone (0.0031, 0.00625, 0.0125, 0.025 mg/kg/infusion) under the same experimental conditions, except that different oxycodone concentrations were available at each unit dose. After stable oxycodone self-administration was achieved, the animals received systemic administration of *R*-VK4-40 (10, 20 mg/kg, i.p.) or vehicle 30 min prior to self-administration sessions.

Experiment 5: Effects of R-VK4-40 on oxycodone self-administration under PR reinforcement

After completing oxycodone dose-response functions as indicated above, animals were switched to a PR schedule of reinforcement, during which the work requirement (lever presses) needed to receive a single i.v. oxycodone infusion was progressively raised within each test session according to the following PR series: 1, 2, 4, 6, 9, 12, 15, 20, 25, 32, 40, 50, 62, 77, 95, 118, 145, 178, 219, 268, 328, 402, 492, and 603, until a break-point was reached. Break-points were defined as the maximal work load (lever presses) completed to earn an oxycodone infusion prior to a 1-h period during which no additional infusion was obtained by the animal. Animals continued daily sessions of oxycodone self-administration under PR reinforcement until variability in break-points was within 1–2 ratio increments for three consecutive days. Once a stable baseline break-point was established, animals were assigned to three subgroups to determine the effects of vehicle and two different doses of *R*-VK4-40 (10, 20 mg/kg, i.p.) on PR break-points.

Experiment 6: Effects of R-VK4-40 on oxycodone-enhanced optical brain-stimulation reward

Surgeries: Male DAT-Cre mice (~4 weeks of age) were anesthetized with ketamine and xylazine and placed in a stereotaxic frame (David Kopf Instruments, Tujunga, CA, USA). For intra-VTA microinjections, a custom-made 30-gauge stainless steel injector was used to infuse Cre-inducible recombinant adeno-associated virus (AAV) that encodes channelrhodopsin-2 (ChR2) and enhanced green fluorescent protein (i.e., AAV-EF1α-DIO-ChR2-EGFP; 150 nl, ~2×10^{12} genomes/ml, University of North Carolina Gene Therapy Center) unilaterally into the VTA (AP −3.28; ML 0.43; DV −4.41 mm relative to Bregma) using a micropump (WPI 2000 UltraMicroPump, Sarasota, FL, USA) with a speed of 50 nl/min. For optical brain stimulation, a custom-built optrode (200-μm multimode optical fiber, Thorlabs, Newton, NJ, USA) fastened to an intracranial ceramic ferrule (MM-FER2007C-2300, Precision Fiber Products, Inc., Milpitas, CA, USA) was implanted into the VTA (AP −3.28; ML 0.43, DV −4.31 mm relative to Bregma) above the AAV injection site. Dental cement was used to fix the optrode assembly to the skull. Following AAV vector injection and optrode implantation, mice were recovered for at least 4 weeks, to enable full AAV expression and ChR2 trafficking, before optical self-stimulation experiments began.

Optical intracranial self-stimulation (oICSS) apparatus: Optical stimulation experiments were conducted in standard operant conditioning chambers (Med Associates, Fairfax, VT, USA). Each chamber was equipped with two wall-mounted levers, two cue lights, a house light, and an audio stimulus generator. Mice were gently connected to a cable attached to an optical swivel, which was in turn connected to a 473 nm laser tuned for ChR2 stimulation. Computer software controlled a pulse generator that controlled the lasers.

oICSS Procedure: The procedures for oICSS were the same as reported recently (Han et al., 2017). After 4 weeks of recovery from surgery, mice were placed into operant chambers containing two levers designated active lever or inactive (ENV-307W-CT, Med associates Inc., Fairfax, VT, USA). The optrode implanted into the mouse brain (VTA) was connected to a 473 nm laser (OEM Laser Systems, Inc., Draper, UT, USA) via an optical swivel (Doric Lenses Inc, Quebec, Canada). Animals were initially trained on a FR1 reinforcement schedule; each active lever response led to delivery of a 1-s pulse train of light stimulation (473 nm, 20 mW, 5 ms duration, 25 Hz) accompanied by a 1-s illumination of cue light above the lever. While inactive lever presses were counted, they had no programmed consequence. Each daily training session lasted 60 min.

Rate-frequency oICSS procedure: Following establishment of lever-pressing for oICSS, animals were presented with a series of 6 different stimulation frequencies (100, 50, 25, 10, 5, 1 Hz) in descending order to obtain rate-frequency response curves. Animals were allowed to respond for 10 min per stimulation frequency. The animals were then divided into 3 groups (6-10 mice per group) to observe the effects of oxycodone (0, 0.3, 1.0, 3 mg/kg, i.p.; 5 min prior to testing), *R*-VK4-40 (0, 3, 10 mg/kg, i.p.; 30 min prior to testing) alone, or 1 mg/kg oxycodone with *R*-VK4-40 pretreatment (3, 10 mg/kg, 25 min prior to oxycodone), respectively, on optical ICSS maintained by photostimulation of VTA DA neurons in DAT-Cre mice. Each animal received 3-5 drug injections during the course of oICSS experiments.

After each test, animals received an additional 2-3 days of oICSS re-stabilization until baseline lever responding was reestablished. The order of testing for the various doses of the drugs was counterbalanced. The effects of oxycodone, *R*-VK4-40, or *R*-VK4-40 + oxycodone on oICSS were evaluated by comparing drug-induced changes in active lever presses in DAT-Cre mice.

Experiment 7: Effects of R-VK4-40 on oxycodone-induced antinociceptive response

Nociceptive tests were performed using a hot plate device (Model 39, IITC Life Science Inc., Woodland Hills, CA, USA). Briefly, rats were placed inside a transparent cage on the hot plate, which was pre-heated to 52 (± 0.2) °C. When thermal nociceptive signs such as licking, stomping the hind paw, or jumping from the plate appeared, the rat was immediately removed from the cage. The time interval (sec) from rat being placed on the hotplate to exhibiting the first sign of thermal nociception was measured. The cut-off time for the test was 60 s to avoid tissue damage.

Four groups of rats were used in this experiment (n=7-9/group). Each rat was first habituated to the testing environment for 1 h, followed by placement on the hot plate without treatment to obtain baseline response latencies. To determine the impact of *R*-VK4-40 on oxycodone analgesia, on the following test days 3 groups were pretreated with vehicle or one of two *R*-VK4-40 doses (10 or 20 mg/kg, i.p.) 30 min prior to one of four doses of oxycodone (0.5, 1, 2, or 4 mg/kg, i.p.). Fifteen minutes after oxycodone injection each rat was tested on the hot plate. To determine the effects of *R*-VK4-40 and oxycodone alone on hot plate analgesia, one group of rats was pretreated with the vehicle, oxycodone (2 mg/kg, i.p.) or one of two *R*-VK4-40 doses (10, 20 mg/kg, i.p.). The hot plate test was then conducted 30, 60, 90 and 120 min after drug injection. Each animal was tested 1-3 times with 24-h intervals. Data were calculated as maximum percentage effect (% MPE) using the formula: (treatment value – baseline value)/(cutoff value – baseline value) × 100. The doses of oxycodone and the time points for the hot plate test were chosen based on our previous reports that the peak effects of oxycodone appeared approximately 30 min following injection (You et al., 2018).

Experiment 8: Effects of R-VK4-40 on sucrose self-administration

Sucrose self-administration was conducted as described previously (Song et al., 2012) in a new group of wild-type C57BL/6J mice (n=12). To facilitate acquisition of sucrose selfadministration, mice were food restricted to 90% body weight for the first week of training. Thereafter mice were fed ad libitum. Active lever presses led to the delivery of 0.02 mL of 5% sucrose solution in a food tray mounted on the operant chamber wall. Sessions were 1-hr in length. After stable baselines were established under ad libitum feeding conditions (stability was defined as less than 20% variability in reinforcers earned across consecutive sessions and an active/inactive lever press ratio exceeding 2:1), mice were pre-treated with one of 2 doses of *R*-VK4-40 (3, or 10 mg/kg, i.p.) or vehicle 30-min prior to the self-administration session.

Experiment 9: Effects of R-VK4-40 on locomotion

Two locomotor experiments were designed to observe the effects of *R*-VK4-40 on locomotor activity. In the first assay, one group of rats (n=8) was placed in open-field locomotor

chambers (Accuscan, Columbus, OH, USA) and habituated for 1 h. After 2-3 days of habituation, each animal randomly received vehicle or one dose of *R*-VK4-40 (10, 20 mg/kg, i.p.) with 24-h intervals. Following each injection, locomotor activity was recorded for an additional 2 h in 10 min bins, and the distance traveled was used to evaluate the effects of *R*-VK4-40 on locomotor activity.

In the second assay, wild-type mice (n=10) were trained on the rotarod device. Mobility was measured by the latency to fall (seconds) from the rotarod rotating at increasing speed from 4 to 40 rev/min over 5 min. After stable baselines were established (defined as less than 20% variability in latency to fall across at least 3 consecutive sessions), mice were pre-treated with one of 2 doses of *R*-VK4-40 (3 or 10 mg/kg, i.p.) or vehicle 30-min prior to rotarod testing. To determine whether the combination of *R*-VK4-40 and oxycodone altered mobility, mice were then pre-treated with vehicle or 10 mg/kg *R*-VK4-40 30 min prior to oxycodone (1 mg/kg, i.p.), which was administered immediately prior to rotarod testing. For oxycodone studies, data were collected at 30-min. timepoints following oxycodone administration for 2 hr total.

Drugs

R-VK4-40 [(*R*)-*N*-(4-(4-(2-Chloro-3-ethylphenyl)piperazin-1-yl)-3-hydroxybutyl)-1H-indole-2-carboxamide HCl] was synthesized in the Medicinal Chemistry Section, NIDA-IRP, using a modification of the published procedure for the racemate (Kumar et al., 2017). Oxycodone HCl and 2-hydroxypropyl-β-cyclodextrin were purchased from Sigma/RBI (St Louis, MO, USA). Oxycodone was dissolved in physiological saline for i.v. infusions. 2-hydroxypropyl-β-cyclodextrin was dissolved in water to achieve a concentration of 25% and was used as a vehicle for *R*-VK4-40.

Data Analyses

Plasma and brain concentrations of *R*-VK4-40 were analyzed using non-compartmental method as implemented in the computer software program Phoenix® WinNonlin® version 7.0 (Certara USA, Inc., Princeton, NJ). The maximum plasma and tissue concentration (C_{max}) and time to C_{max} (T_{max}) were the observed values. The area under the plasma and tissue concentration time curve (AUC) value was calculated up to 8 h (AUC_{0-t}) by use of the log-linear trapezoidal rule. Brain to plasma ratio is calculated from mean total AUC_{brain} versus AUC_{plasma}.

All behavioral data are presented as means ± SEM. One-way or two-way analyses of variance (ANOVAs) with repeated measures over time or dose were used to analyze data across experiments. Post-hoc multiple comparisons were carried out using the Tukey test. $p<0.05$ was considered to indicate statistical significance.

RESULTS

R-VK4-40 is a novel highly potent and selective D_3R antagonist

Figure 1 shows the chemical structures and *in vitro* binding affinities of *R*-VK4-40 compared to previously reported D_3R antagonists/partial agonists CAB2-015, BAK4-54 and

(±)VK4-116 (Kumar et al., 2016; You et al., 2017). Compared to CAB2-015 and BAK4-54, *R*-VK4-40 shows comparably high affinity for D_3R (K_i0.290 nM) and is more selective (261-fold) over D_2R (K_i = 75.8 nM, Figure 1).

R-VK4-40 is metabolically stable in rat liver microsomes

Figure 2 shows the phase I metabolic stability of *R*-VK4-40 in rat liver microsomes fortified with NADPH. *R*-VK4-40 showed stability to phase I metabolism with 86±2 % intact remaining following 60 min incubation. Negative control without cofactors showed complete stability in rat liver microsomes. Buprenorphine was used as a positive control and <1% compound remained at 60 min. Overall the results suggest compound undergoes limited CYP dependent metabolism, and would will undergo minimal hepatic first pass effects upon oral administration.

R-VK4-40 shows oral availability and brain penetration in rats

Figure 3 shows pharmacokinetic evaluation conducted in rats following oral administration at 10 mg/kg. *R*-VK4-40 was orally available achieving a maximum concentration (C_{max} = 0.31 ± 0.11 nmol/mL) at 4 h post dose. The plasma $AUC_{0\text{-}t}$ was 1.99 ± 0.28 nmol.h/mL. Notably, in brain the maximum concentration achieved (C_{max}= 3.85 ± 0.51 nmol/g) were ~12 fold higher relative to plasma. Similarly, the overall brain exposures ($AUC_{0\text{-}t}$= 21.6 ± 1.41 nmol.h/g) were 10.8 fold higher relative to plasma, suggesting excellent brain penetration.

R-VK4-40 inhibits oxycodone self-administration under FR1 reinforcement

As reported previously (You et al., 2017), experimental rats displayed a typical inverted U-shaped curve of oxycodone self-administration (infusions earned) across a full range of oxycodone doses (Figure 4A). Pretreatment with *R*-VK4-40 produced a dose-dependent reduction in oxycodone self-administration, indicated by a downward shift of the oxycodone dose-response curve. Two-way ANOVA with repeated measures for oxycodone dose revealed significant treatment main effects ($F_{2,214}$=10.79, p<0.001). Post-hoc individual group comparisons revealed that *R*-VK4-40 significantly reduced infusions earned at multiple oxycodone doses (Figure 4A). Figure 4B shows the daily oxycodone intake (mg/kg) during self-administration maintained by different unit doses of oxycodone. Two-way ANOVA revealed significant main effects of treatment ($F_{2,99}$ = 5.68, p<0.01), dose ($F_{4,99}$ = 4.26, p<0.01), and a treatment × dose interaction ($F_{8,99}$ = 4.82, p<0.001). Post-hoc testing indicated that *R*-VK4-40 reduced oxycodone intake at the 0.00625 and 0.05 mg/kg doses (Figure 4B). Figure 4C shows that pretreatment with *R*-VK4-40 had no effect on inactive lever responding.

R-VK4-40 pretreatment lowers break-points for oxycodone self-administration under PR reinforcement

To determine whether the reduction in oxycodone self-administration reported above was due to a reduction in oxycodone's rewarding efficacy, we further trained animals to self-administer oxycodone under PR reinforcement and observed the effects of *R*-VK4-40 on break-point, an index of reward strength (Xi et al., 2005). Figure 5A shows that systemic

administration of *R*-VK4-40 significantly lowered break-points for oxycodone self-administration in a dose-dependent manner. However, one-way ANOVA did not reveal statistically significant effects ($F_{2,31} = 2.04$, $p>0.05$), in part due to variability across individual animals. We therefore normalized break-points following vehicle or *R*-VK4-40 treatment as a percentage of baseline for each animal (Figure 5B). One-way ANOVA then revealed that pretreatment with *R*-VK4-40 significantly reduced PR break-points for oxycodone self-administration (Figure 5B, one-way ANOVA, $F_{2,31} = 3.66$, $p<0.05$). Post-hoc analyses indicated a significant decrease in break-point after 20 mg/kg *R*-VK4-40 treatment compared to the vehicle-treated group. These findings suggest D_3R antagonism by *R*-VK4-40 reduces oxycodone reward.

R-VK4-40 blocks oxycodone-enhanced optical brain-stimulation reward

To determine whether a DA-dependent mechanism underlies the reduction in oxycodone reward reported above, we next observed the effects of *R*-VK4-40 on intracranial self-stimulation (ICSS) maintained by optical activation of VTA DA neurons in DAT-Cre mice. Figure 6A depicts experimental procedures, illustrating microinjection of AAV-DIO-ChR2-EGFP unilaterally into the VTA in DAT-Cre mice, with an optical fiber implanted into the VTA above the injection site. Figure 6 (B, C, D) shows representative tyrosine hydroxylase (TH)-immunostaining and fluorescent EGFP images, illustrating DAT promoter-driven ChR2-EGFP expression within the VTA. Figure 6 (E, F, G, H) shows the results of optical intracranial selfstimulation (oICSS) in the absence or presence of oxycodone and/or *R*-VK4-40. In the vehicle control groups, response-contingent photoactivation of VTA DA neurons induced robust active lever presses in a stimulation frequency-dependent manner – the higher the stimulation frequency, the more the active lever presses, and *vice versa*. These findings suggest that photostimulation of VTA DA neurons is reinforcing.

We then examined whether oxycodone, *R*-VK4-40, or *R*-VK4-40 pretreatment prior to oxycodone alters oICSS responding. Figure 6F shows that systemic administration of oxycodone (0.3, 1.0, 3.0 mg/kg, i.p., 5 min prior to testing) produced biphasic effects – lower doses enhanced, while a higher dose decreased optical brain-stimulation reward as assessed by upward or downward shifted rate-frequency response curves, respectively. Two-way ANOVA with repeated measures for oxycodone dose and stimulation frequency revealed a significant oxycodone treatment main effect (Figure 6F: $F_{3,180,180} = 10.71$, $p<0.001$). Post-hoc individual group comparisons revealed a significant increase in oICSS after 1 mg/kg oxycodone and a significant reduction in oICSS after 3 mg/kg oxycodone compared to vehicle control group ($p<0.05$). Figure 6G shows the effects of *R*-VK4-40 (10, 20 mg/kg) alone, indicating that *R*-VK4-40 produced a significant reduction in oICSS and shifted the rate-frequency function curve downward and rightward. Two-way ANOVA with repeated measures for *R*-VK4-40 dose and stimulation frequency revealed a statistically significant *R*-VK4-40 treatment main effect (Fig. 6G: $F_{2,102} = 14.29$, $p<0.001$). Strikingly, pretreatment with *R*-VK4-40 significantly reduced low-dose (1 mg/kg) oxycodone enhancements in oICSS in a dose-dependent manner (Fig. 6H, two-way ANOVA, main dose effect $F_{2,102} = 39.64$,$p<0.001$; dose × frequency interaction $F_{5,102}=12.24$, $p<0.001$), suggesting that a DA-dependent mechanism underlies the interaction of *R*-VK4-40 and oxycodone in brain reward function (but see rotarod report, below).

R-VK4-40 does not diminish oxycodone's antinociceptive effects in rats

To determine whether pretreatment with or co-administration of a D_3R antagonist compromises the therapeutic analgesic effects of opioids, we observed the effects of *R*-VK4-40 and/or oxycodone on animals' thermal nociceptive responses in the hot-plate test. Figure 7A shows the time course of the effects of *R*-VK4-40 or oxycodone alone on hot plate nociception. Oxycodone produced a robust antinociceptive effect, as indicated by increased latency in thermal nociceptive response, with a peak effect at 30 min after oxycodone administration. Strikingly, *R*-VK4-40 also produced a dose-dependent antinociceptive effect over time (Figure 7A). Two-way ANOVA indicates that the statistical significance of oxycodone- or *R*-VK4-40-induced increases in latency to thermal nociceptive response ($F_{3,117} = 4.39$, $p<0.01$).

We then observed the effects of *R*-VK4-40 pretreatment on oxycodone analgesia. Figure 7B shows the effects of *R*-VK4-40 pretreatment on the dose-response curve of oxycodone-induced analgesia. *R*-VK4-40 pretreatment shifted the oxycodone dose-response curve significantly upward. Two-way ANOVA revealed significant main effects of *R*-VK4-40 ($F_{2,60} = 7.6$, $p<0.01$) and oxycodone dose ($F_{3,60} = 43.47$,$p<0.001$), and a non-significant treatment × dose interaction ($F_{6,91}= 0.65$, $p=0.68$). Post-hoc individual group comparisons indicated that *R*-VK4-40, at 20 mg/kg, produced a significant elevation of %MPE after 1 mg/kg oxycodone administration ($p<0.05$).

R-VK4-40 attenuates sucrose self-administration

We next sought to determine whether *R*-VK4-40 alters responding for non-drug reward. Figure 7C shows the impact of *R*-VK4-40 on the number of sucrose reinforcers earned by mice. Oneway ANOVA revealed a significant main effect of treatment ($F_{2,22} = 28.6$, $p<0.001$). Post-hoc testing indicated that 10 mg/kg *R*-VK4-40 significantly reduced the number of sucrose reinforcers earned compared to vehicle and 3 mg/kg *R*-VK4-40 ($p<0.001$). There were no statistically significant differences between vehicle and 3 mg/kg *R*-VK4-40.

R-VK4-40 has no effect on locomotor behavior

Finally, we examined whether the effects of *R*-VK4-40 on oxycodone self-administration, oICSS or thermal nociceptive responses are due to locomotor impairment. Figure 7D shows that systemic administration of *R*-VK4-40 (10 or 20 mg/kg, i.p.) had no effect on open-field locomotion in rats compared to the vehicle control group (main effect of dose: $F_{2,378} = 0.72$, $p=0.99$). Figure 7E shows the impact of *R*-VK4-40 alone on rotarod mobility in mice. One-way ANOVA revealed no statistically significant impact of treatment on latency to fall. Figure 7F shows the impact of a high dose of *R*-VK-40 in combination with oxycodone on rotarod mobility over 2 hrs. Two-way ANOVA revealed a main effect of time ($F_{4,26} = 3.7$, $p<0.01$), but not treatment or its interaction with time. To further examine these data, we re-conducted statistical analyses without the 2-hr timepoint (i.e., 0-90 min data only). Two-way ANOVA revealed a significant treatment effect ($F_{1,27} = 8.9$, $p<0.01$) and a trend towards a main effect of time ($F_{3,27} = 2.7$, $p=0.06$), but not a significant treatment × time interaction. These results suggest that the differences in fall latency between the two groups are not statistically significant.

DISCUSSION

In this study, we systematically examined the effects of D_3R blockade by VK4-40 on opioid reward. We found that *R*-VK4-40, a highly selective and metabolically stable D_3R antagonist, produced a dose-dependent reduction in oxycodone self-administration under FR1 and PR reinforcement schedules. In addition, *R*-VK4-40 inhibited olCSS maintained by optogenetic activation of VTA DA neurons, and blocked oxycodone-enhanced brain-stimulation reward. Strikingly, during the hot plate assay *R*-VK4-40 alone produced analgesia at two-hours postinjection that mimicked the effectiveness of oxycodone alone at 30-minutes post-injection, suggesting that *R*-VK4-40 may be as efficacious as oxycodone in promoting analgesia but with a slower onset of action. Together, these results suggest that co-administration of *R*-VK4-40 with opioid analgesics may produce similar pain-relieving effects as those produced by higher opioid doses, which are possibly longer lasting. The behavioral effects of *R*-VK4-40 are unlikely to have been due to nonspecific motor impairment since *R*-VK4-40 treatment affected neither locomotor activity in an open field nor on the rotarod test.

The observation that *R*-VK4-40 inhibits oxycodone self-administration is consistent with previous reports that D_3R blockade by SB-277011A or other D_3R antagonists significantly inhibits opioid-induced conditioned place preferences (CPP) in rats (Ashby et al., 2003), heroin self-administration in wildtype, but not in D_3R-knockout mice (Boateng et al., 2015), and oxycodone self-administration in rats (You et al., 2017). Opioid reward is generally believed to be mediated by activation of mu opioid receptors located on GABAergic interneurons or afferents in the VTA, which subsequently disinhibit VTA DA neurons (Fields and Margolis, 2015). Given 1) the critical role of DA in drug reward and 2) that D_3R has the highest affinity for DA of all DA receptors, we hypothesized that blockade of D_3Rs would attenuate DA-mediated effects such as opioid reward. To test this hypothesis, we used state-of-the-art transgenic and optogenetic approaches to selectively activate VTA DA neurons and observed behavioral responding for brain stimulation. Classically, addictive drugs produce additive or synergistic effects on the brain DA system and reward function (Bauco and Wise, 1997; Peng et al., 2010; Wise, 1996; Xi and Gardner, 2007). However, in the present study oxycodone produced biphasic effects – low doses enhanced, while higher doses inhibited oICSS, as assessed by upward/leftward or rightward/downward shifts in rate-frequency response curves, respectively. These shifts are consistent with reports in both humans and experimental animals that low doses of opioids are rewarding and high doses of opioids are aversive (Herz, 1988; Jensen, 1997).

Although the GABA-DA hypothesis of opioid reward is well-accepted (Fields and Margolis, 2015), other reports indicate that mu opioid receptors may be expressed in both GABAergic and DA neurons of the VTA, such that opioids may directly inhibit a subset of VTA DA neurons (Cameron et al., 1997; Ford et al., 2006; Margolis et al., 2014). Mu opioid receptor activation on VTA GABAergic neurons or afferents may underlie low dose opioid-mediated oICSS reward, whereas mu activation on VTA DA neurons by higher doses of oxycodone may produce oICSS aversion via inhibition of DA release. Therefore, the potentiation of ICSS induced by low dose of oxycodone may be mediated indirectly by mu receptors located on VTA GABA neurons and GABAergic afferents, while the effects produced by the

high dose of oxycodone may represent direct impact of oxycodone on VTA DA neurons. Clearly, more studies are required to test this hypothesis. Another alternative may be that high doses of oxycodone activate kappa opioid receptors located on VTA DA neurons and/or DA terminals in the nucleus accumbens, producing aversion (Wee and Koob, 2010). In addition, high doses of opioids are known to suppress locomotor activity, which may in part contribute to the reduction in oICSS responding. Regardless of the mechanisms underlying oxycodone action on oICSS, as hypothesized, blockade of D_3Rs by *R*-VK4-40 significantly inhibited oICSS and oxycodone-enhanced oICSS, suggesting an essential role of D_3Rs in DA-mediated reward. This finding is consistent with our recent report that genetic deletion of D_3Rs in D_3-knockout mice attenuates mesolimbic DA and locomotor responses to heroin (Zhan et al., 2018), and supports D_3R antagonist treatment as an effective adjunctive medication to reduce the abuse liability of prescription opioids.

In addition to impacting opioid reward, *R*-VK4-40 also attenuated sucrose selfadministration at the higher dose tested in mice, suggesting D_3R involvement in non-drug reward. Literature reports regarding the pharmacological action of D_3R antagonists on sucrose or food-taking behavior are mixed. Several studies show that the D_3R antagonists (SB-277011A, YQA14, BAK-4-54; VK4-116) have no significant effect on sucrose self-administration or on food-induced conditioned place preference (Song et al., 2012; Vorel et al., 2002; You et al., 2018; You et al., 2017), while others report that D_3R antagonists (SB-277011A, PG01037, NGB-2904, GSK598809, CAB2-015) or a partial agonist (FAUC 329) significantly inhibit food-taking and food-seeking behavior (Higley et al., 2011; Maramai et al., 2016; Nathan et al., 2012; Stossel et al., 2017; Thanos et al., 2008; Thomsen et al., 2017; You et al., 2017). The mechanisms underlying these inconsistent findings are unclear. One possibility is that, at high doses, D_3R antagonists may bind to D_2R, which has a known role in food-taking and food reward (Soto et al., 2016; Thomsen et al., 2017) or other off-targets may be involved. Another possibility is that food and drugs of abuse activate common neural circuits within the mesolimbic DA reward system. Accordingly, blockade of D_3R within the mesolimbic system would be expected to inhibit food- and drug-taking behaviors. This interpretation suggests that R-VK4-40 or other D_3R antagonists may have therapeutic potential in controlling binge-eating and the development of obesity (Mogg et al., 2012; Nathan et al., 2012; Thanos et al., 2008).

Importantly, *R*-VK4-40, at doses that inhibited oxycodone self-administration, did not compromise the therapeutic antinociceptive effects of oxycodone. Rather, *R*-VK4-40 alone produced significant analgesic effects over the course of two hours, and pretreatment with *R*-VK4-40 dose-dependently enhanced the increased hot plate latencies produced by oxycodone. This enhancement is unlikely due to locomotor impairment since co-administration of R-VK4-40 and oxycodone did not produce a statistically significant effect on locomotor performance in the rotarod test. Similarly, D_3R deletion in knockout mice causes hypoalgesia, as assessed by increased paw withdrawal latencies to thermal pain stimulation (Li et al., 2012; Zhu et al., 2010). Co-administration of *R*-VK4-40 alongside prescription opioids may therefore augment opioids' clinical utility. *R*-VK4-40 could potentially minimize prescription of escalating doses of oxycodone, which convey side effects such as tolerance, dependence, and overdose due to respiratory suppression.

The mechanisms underlying D3R antagonist-mediated analgesia are unknown. Activation of D_1 and D_2 receptors in pain-related brain regions such as the periaqueductal gray (PAG) produces antinociceptive effects (Magnusson and Fisher, 2000; Meyer et al., 2009). Blockade of D_3Rs by NGB2904, another selective D_3R antagonist, enhanced cocaine-induced increases in extracellular nucleus accumbens DA, possibly via a presynaptic D_3R mechanism (Xi and Gardner, 2007). We expect that a DA-dependent mechanism may also be involved in D_3R-mediated analgesia, but further studies are required to investigate this hypothesis.

In summary, blockade of D_3Rs by the novel D_3R antagonist, *R*-VK4-40, inhibits opioid reward and augments opioid analgesia via DA-dependent mechanisms, suggesting high translational potential. Together, these findings support further development of *R*-VK4-40 as a pharmacotherapeutic agent for the treatment and prevention of prescription opioid abuse.

Acknowledgments

Funding and Disclosures: This research was supported by NIDA-IRP (Z1A DA000424). None of the authors have any disclosures. A.H.N. and A.B.S. are co-inventors on an NIH patent that covers *R*-VK4-40. All rights are reserved by NIH.

References

Andreoli M, Tessari M, Pilla M, Valerio E, Hagan JJ, Heidbreder CA. 2003 Selective antagonism at dopamine D3 receptors prevents nicotine-triggered relapse to nicotineseeking behavior. Neuropsychopharmacology 28: 1272–80. [PubMed: 12700694]

Ashby CR Jr., Paul M, Gardner EL, Heidbreder CA, Hagan JJ 2003 Acute administration of the selective D3 receptor antagonist SB-277011A blocks the acquisition and expression of the conditioned place preference response to heroin in male rats. Synapse 48: 154–6. [PubMed: 12645041]

Aujla H, Beninger RJ. 2005 The dopamine D(3) receptor-preferring partial agonist BP 897 dose-dependently attenuates the expression of amphetamine-conditioned place preference in rats. Behav Pharmacol 16: 181–6. [PubMed: 15864073]

Bauco P, Wise RA. 1997 Synergistic effects of cocaine with lateral hypothalamic brain stimulation reward: lack of tolerance or sensitization. J Pharmacol Exp Ther 283: 1160–7. [PubMed: 9399989]

Boateng CA, Bakare OM, Zhan J, Banala AK, Burzynski C, et al. 2015 High Affinity Dopamine D3 Receptor (D3R)-Selective Antagonists Attenuate Heroin Self-Administration in Wild-Type but not D3R Knockout Mice. J Med Chem 58: 6195–213. [PubMed: 26203768]

Cameron DL, Wessendorf MW, Williams JT. 1997 A subset of ventral tegmental area neurons is inhibited by dopamine, 5-hydroxytryptamine and opioids. Neuroscience 77: 155–66. [PubMed: 9044383]

Compton WM, Jones CM, Baldwin GT. 2016 Relationship between Nonmedical Prescription-Opioid Use and Heroin Use. N Engl J Med 374: 154–63. [PubMed: 26760086]

Fields HL, Margolis EB. 2015 Understanding opioid reward. Trends Neurosci 38: 217–25. [PubMed: 25637939]

Ford CP, Mark GP, Williams JT. 2006 Properties and opioid inhibition of mesolimbic dopamine neurons vary according to target location. J Neurosci 26: 2788–97. [PubMed: 16525058]

Galaj E, Manuszak M, Babic S, Ananthan S, Ranaldi R. 2015 The selective dopamine D3 receptor antagonist, SR 21502, reduces cue-induced reinstatement of heroin seeking and heroin conditioned place preference in rats. Drug Alcohol Depend 156: 228–33. [PubMed: 26429728]

Gilbert JG, Newman AH, Gardner EL, Ashby CR Jr., Heidbreder CA, et al. 2005 Acute administration of SB-277011A, NGB 2904, or BP 897 inhibits cocaine cue-induced reinstatement of drug-seeking behavior in rats: role of dopamine D3 receptors. Synapse 57: 17–28. [PubMed: 15858839]

Han X, He Y, Bi GH, Zhang HY, Song R, et al. 2017 CB1 Receptor Activation on VgluT2-Expressing Glutamatergic Neurons Underlies Delta(9)-Tetrahydrocannabinol (Delta(9)-THC)-Induced Aversive Effects in Mice. Sci Rep 7: 12315. [PubMed: 28951549]

Heidbreder CA, Newman AH. 2010 Current perspectives on selective dopamine D(3) receptor antagonists as pharmacotherapeutics for addictions and related disorders. Ann N Y Acad Sci 1187: 4–34. [PubMed: 20201845]

Herz A 1988 Bidirectional effects of opioids in motivational processes and the involvement of D1 dopamine receptors. NIDA Res Monogr 90: 17–26. [PubMed: 2855853]

Higley AE, Kiefer SW, Li X, Gaal J, Xi ZX, Gardner EL. 2011 Dopamine D(3) receptor antagonist SB-277011A inhibits methamphetamine self-administration and methamphetamine-induced reinstatement of drug-seeking in rats. Eur J Pharmacol 659: 187–92. [PubMed: 21466803]

Jensen TS. 1997 Opioids in the brain: supraspinal mechanisms in pain control. Acta Anaesthesiol Scand 41: 123–32. [PubMed: 9061095]

Jones CM, Einstein EB, Compton WM. 2018 Changes in Synthetic Opioid Involvement in Drug Overdose Deaths in the United States, 2010-2016. JAMA 319: 1819–21. [PubMed: 29715347]

Keck TM, John WS, Czoty PW, Nader MA, Newman AH. 2015 Identifying Medication Targets for Psychostimulant Addiction: Unraveling the Dopamine D3 Receptor Hypothesis. J Med Chem 58: 5361–80. [PubMed: 25826710]

Kenan K, Mack K, Paulozzi L. 2012 Trends in prescriptions for oxycodone and other commonly used opioids in the United States, 2000-2010. Open Med 6: e41–7. [PubMed: 23696768]

Kumar V, Bonifazi A, Ellenberger MP, Keck TM, Pommier E, et al. 2016 Highly Selective Dopamine D3 Receptor (D3R) Antagonists and Partial Agonists Based on Eticlopride and the D3R Crystal Structure: New Leads for Opioid Dependence Treatment. J Med Chem 59: 7634–50. [PubMed: 27508895]

Kumar V, Moritz AE, Keck TM, Bonifazi A, Ellenberger MP, et al. 2017 Synthesis and Pharmacological Characterization of Novel trans-Cyclopropylmethyl-Linked Bivalent Ligands That Exhibit Selectivity and Allosteric Pharmacology at the Dopamine D3 Receptor (D3R). J Med Chem 60: 1478–94. [PubMed: 28186762]

Li T, Hou Y, Cao W, Yan CX, Chen T, Li SB. 2012 Role of dopamine D3 receptors in basal nociception regulation and in morphine-induced tolerance and withdrawal. Brain Res 1433: 80–4. [PubMed: 22154407]

Magnusson JE, Fisher K. 2000 The involvement of dopamine in nociception: the role of D(1) and D(2) receptors in the dorsolateral striatum. Brain Res 855: 260–6. [PubMed: 10677598]

Maramai S, Gemma S, Brogi S, Campiani G, Butini S, et al. 2016 Dopamine D3 Receptor Antagonists as Potential Therapeutics for the Treatment of Neurological Diseases. Front Neurosci 10: 451. [PubMed: 27761108]

Margolis EB, Hjelmstad GO, Fujita W, Fields HL. 2014 Direct bidirectional mu-opioid control of midbrain dopamine neurons. J Neurosci 34: 14707–16. [PubMed: 25355223]

Meyer PJ, Morgan MM, Kozell LB, Ingram SL. 2009 Contribution of dopamine receptors to periaqueductal gray-mediated antinociception. Psychopharmacology (Berl) 204: 531–40. [PubMed: 19225762]

Meyer R, Patel AM, Rattana SK, Quock TP, Mody SH. 2014 Prescription opioid abuse: a literature review of the clinical and economic burden in the United States. Popul Health Manag 17: 372–87. [PubMed: 25075734]

Micheli F, Bonanomi G, Blaney FE, Braggio S, Capelli AM, et al. 2007 1,2,4-triazol-3-yl-thiopropyl-tetrahydrobenzazepines: a series of potent and selective dopamine D(3) receptor antagonists. J Med Chem 50: 5076–89. [PubMed: 17867665]

Mogg K, Bradley BP, O'Neill B, Bani M, Merlo-Pich E, et al. 2012 Effect of dopamine D(3) receptor antagonism on approach responses to food cues in overweight and obese individuals. Behav Pharmacol 23: 603–8. [PubMed: 22772335]

Nathan PJ, O'Neill BV, Mogg K, Bradley BP, Beaver J, et al. 2012 The effects of the dopamine D(3) receptor antagonist GSK598809 on attentional bias to palatable food cues in overweight and obese subjects. Int J Neuropsychopharmacol 15: 149–61. [PubMed: 21745436]

Novick DM, Salsitz EA, Joseph H, Kreek MJ. 2015 Methadone Medical Maintenance: An Early 21st-Century Perspective. J Addict Dis 34: 226–37. [PubMed: 26110221]

Pak AC, Ashby CR Jr., Heidbreder CA, Pilla M, Gilbert J, et al. 2006 The selective dopamine D3 receptor antagonist SB-277011A reduces nicotine-enhanced brain reward and nicotine-paired environmental cue functions. Int J Neuropsychopharmacol 9: 585–602. [PubMed: 16942635]

Peng XQ, Xi ZX, Li X, Spiller K, Li J, et al. 2010 Is slow-onset long-acting monoamine transport blockade to cocaine as methadone is to heroin? Implication for anti-addiction medications. Neuropsychopharmacology 35: 2564–78. [PubMed: 20827272]

Ross JT, Corrigall WA, Heidbreder CA, LeSage MG. 2007 Effects of the selective dopamine D3 receptor antagonist SB-277011A on the reinforcing effects of nicotine as measured by a progressive-ratio schedule in rats. Eur J Pharmacol 559: 173–9. [PubMed: 17303116]

Sokoloff P, Le Foll B. 2017 The dopamine D3 receptor, a quarter century later. Eur J Neurosci 45: 2–19. [PubMed: 27600596]

Song R, Yang RF, Wu N, Su RB, Li J, et al. 2012 YQA14: a novel dopamine D3 receptor antagonist that inhibits cocaine self-administration in rats and mice, but not in D3 receptor-knockout mice. Addict Biol 17: 259–73. [PubMed: 21507153]

Song R, Zhang HY, Peng XQ, Su RB, Yang RF, et al. 2013 Dopamine D(3) receptor deletion or blockade attenuates cocaine-induced conditioned place preference in mice. Neuropharmacology 72: 82–7. [PubMed: 23643749]

Soto PL, Hiranita T, Xu M, Hursh SR, Grandy DK, Katz JL. 2016 Dopamine D(2)-Like Receptors and Behavioral Economics of Food Reinforcement. Neuropsychopharmacology 41: 971–8. [PubMed: 26205210]

Spiller K, Xi ZX, Peng XQ, Newman AH, Ashby CR Jr., et al. 2008 The selective dopamine D3 receptor antagonists SB-277011A and NGB 2904 and the putative partial D3 receptor agonist BP-897 attenuate methamphetamine-enhanced brain stimulation reward in rats. Psychopharmacology (Berl) 196: 533–42. [PubMed: 17985117]

Stossel A, Brox R, Purkayastha N, Hubner H, Hocke C, et al. 2017 Development of molecular tools based on the dopamine D3 receptor ligand FAUC 329 showing inhibiting effects on drug and food maintained behavior. Bioorg Med Chem 25: 3491–99. [PubMed: 28495386]

Thanos PK, Michaelides M, Ho CW, Wang GJ, Newman AH, et al. 2008 The effects of two highly selective dopamine D3 receptor antagonists (SB-277011A and NGB-2904) on food self-administration in a rodent model of obesity. Pharmacol Biochem Behav 89: 499–507. [PubMed: 18329700]

Thomsen M, Barrett AC, Butler P, Negus SS, Caine SB. 2017 Effects of Acute and Chronic Treatments with Dopamine D2 and D3 Receptor Ligands on Cocaine versus Food Choice in Rats. J Pharmacol Exp Ther 362: 161–76. [PubMed: 28473458]

Vorel SR, Ashby CR Jr., Paul M, Liu X, Hayes R, et al. 2002 Dopamine D3 receptor antagonism inhibits cocaine-seeking and cocaine-enhanced brain reward in rats. J Neurosci 22: 9595–603. [PubMed: 12417684]

Wee S, Koob GF. 2010 The role of the dynorphin-kappa opioid system in the reinforcing effects of drugs of abuse. Psychopharmacology (Berl) 210: 121–35. [PubMed: 20352414]

Wise RA. 1996 Addictive drugs and brain stimulation reward. Annu Rev Neurosci 19: 319–40. [PubMed: 8833446]

Xi ZX, Gardner EL. 2007 Pharmacological actions of NGB 2904, a selective dopamine D3 receptor antagonist, in animal models of drug addiction. CNS Drug Rev 13: 240–59. [PubMed: 17627675]

Xi ZX, Gilbert J, Campos AC, Kline N, Ashby CR Jr., et al. 2004 Blockade of mesolimbic dopamine D3 receptors inhibits stress-induced reinstatement of cocaine-seeking in rats. Psychopharmacology (Berl) 176: 57–65. [PubMed: 15083257]

Xi ZX, Gilbert JG, Pak AC, Ashby CR Jr., Heidbreder CA, Gardner EL 2005 Selective dopamine D3 receptor antagonism by SB-277011A attenuates cocaine reinforcement as assessed by progressive-ratio and variable-cost-variable-payoff fixed-ratio cocaine self-administration in rats. Eur J Neurosci 21: 3427–38. [PubMed: 16026480]

Xi ZX, Newman AH, Gilbert JG, Pak AC, Peng XQ, et al. 2006 The novel dopamine D3 receptor antagonist NGB 2904 inhibits cocaine's rewarding effects and cocaine-induced reinstatement of drug-seeking behavior in rats. Neuropsychopharmacology 31: 1393–405. [PubMed: 16205781]

You ZB, Bi GH, Galaj E, Kumar V, Cao J, et al. 2018 Dopamine D3R antagonist VK4-116 attenuates oxycodone self-administration and reinstatement without compromising its antinociceptive effects. Neuropsychopharmacology

You ZB, Gao JT, Bi GH, He Y, Boateng C, et al. 2017 The novel dopamine D3 receptor antagonists/partial agonists CAB2-015 and BAK4-54 inhibit oxycodone-taking and oxycodone-seeking behavior in rats. Neuropharmacology 126: 190–99. [PubMed: 28888944]

Zhan J, Jordan CJ, Bi GH, He XH, Gardner EL, et al. 2018 Genetic deletion of the dopamine D3 receptor increases vulnerability to heroin in mice. Neuropharmacology 141: 11–20. [PubMed: 30138692]

Zhu J, Chen Y, Lai J, Dang Y, Yan C, et al. 2010 Dopamine D3 receptor regulates basal but not amphetamine-induced changes in pain sensitivity in mice. Neurosci Lett 477: 134–7. [PubMed: 20433900]

Highlights:

1. *R*-VK4-40 is a novel, highly selective D_3R antagonist
2. *R*-VK4-40 inhibits oxycodone self-administration under FR and PR reinforcement schedules
3. *R*-VK4-40 attenuates oxycodone-enhanced optogenetic brain-stimulation reward
4. *R*-VK4-40 enhances the analgesic effects of oxycodone

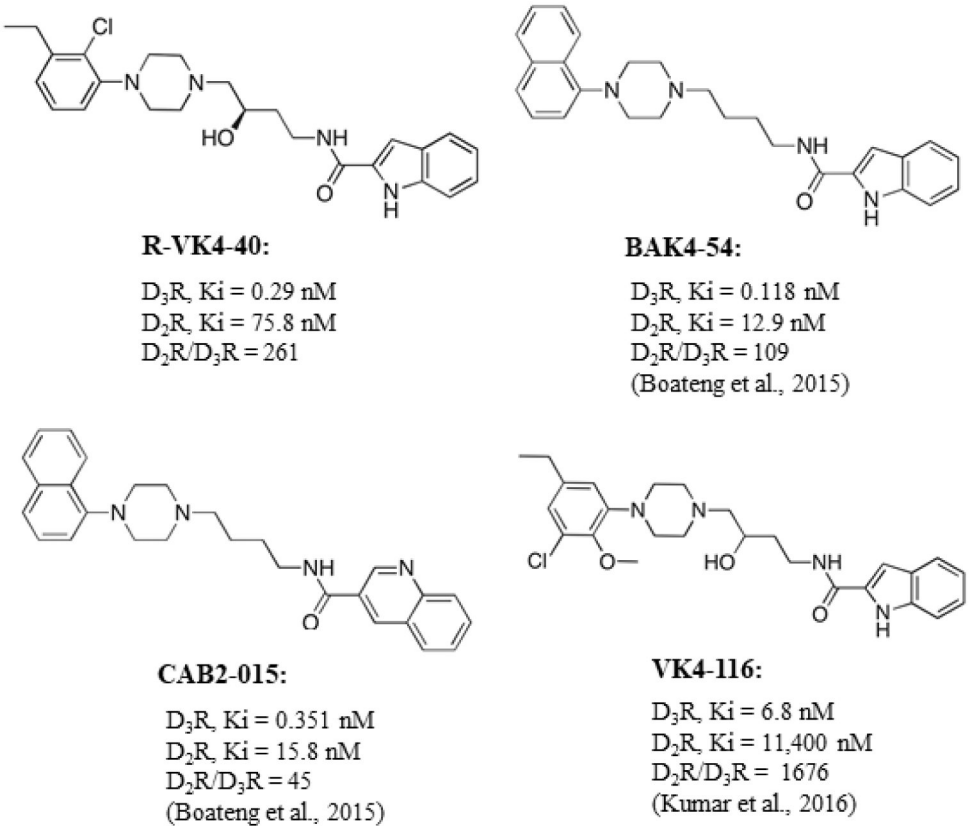

Figure 1.

The chemical structure and receptor binding affinities of *R*-VK4-40 and comparisons to previously reported D_3R antagonists/partial agonists CAB2-015, BAK4-54 and (±)VK4-116.

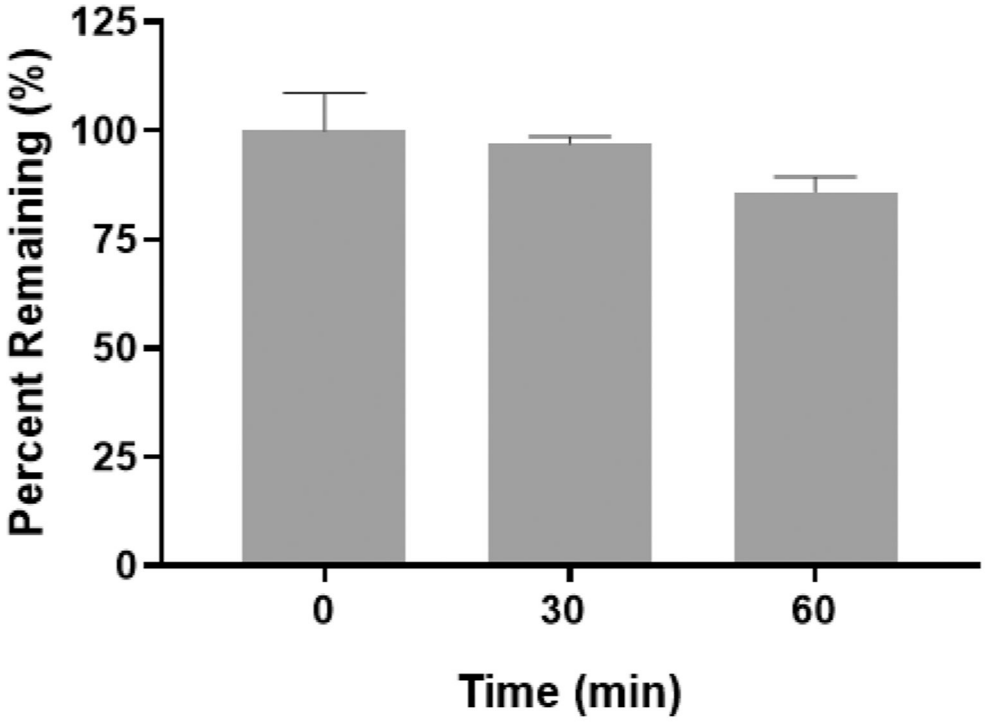

Figure 2.

Phase I metabolic stability of *R*-VK4-40 in rat liver microsomes fortified with NADPH. *R*-VK4-40 was stable in rat liver microsomes with 86 ± 2 % intact remaining following 60 min incubation. Control experiments without cofactors were conducted in parallel with >95% compound remained at 60 min.

A

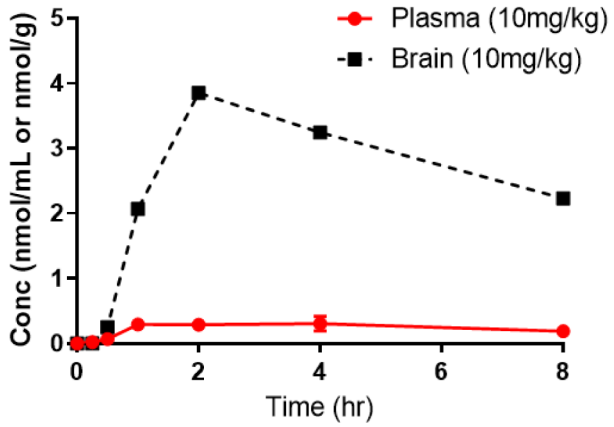

B

Pharmacokinetic Parameters					
Tissue	**Dose (*mg/kg*)**	**C_{max} (*nmol/mL or nmol/g*)**	**T_{max} (*h*)**	**AUC_{0-t} (*nmol.h/mL or nmol.h/g*)**	**AUC_{brain}/AUC_{plasma}**
Plasma	10.0	0.31 ± 0.11	4	1.99 ± 0.28	10.8
Brain		3.85 ± 0.51	2	21.6 ± 1.41	

Figure 3.

Pharmacokinetic evaluation of *R*-VK4-40 following peri-oral administration in rats at 10 mg/kg. (A) Plasma and brain concentration vs time profile of *R*-VK4-40; data is expressed as mean ± SD, n=3, per time-point. (B) Mean ± SD pharmacokinetic parameters in plasma and brain. Brain to plasma ratio is calculated from mean total AUC_{brain} to AUC_{plasma}.

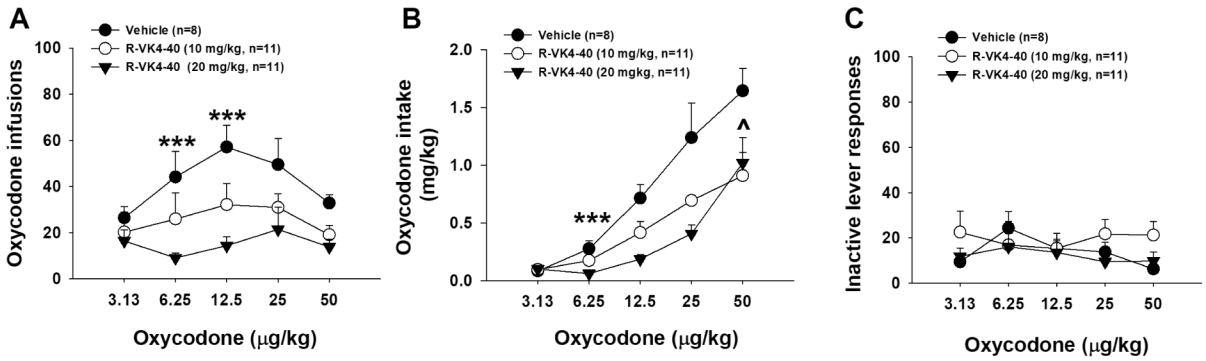

Figure 4.

Effects of *R*-VK4-40 on oxycodone self-administration under FR1 reinforcement in rats. ***A:*** Oxycodone self-administration dose-response curves in the presence or absence of *R*-VK4-40, illustrating that *R*-VK4-40 dose-dependently inhibited oxycodone self-administration. ***B:*** Pretreatments with R-VK4-40 also dose-dependently reduced oxycodone intake (mg/kg) during self-administration. ***C:*** Pretreatment with *R*-VK4-40 had no effect on inactive lever responses during oxycodone self-administration. *p*å<0.01 (10 mg/kg *R*-VK4-40), ***$p<0.001$ (20 mg/kg *R*-VK4-40) compared to vehicle group.

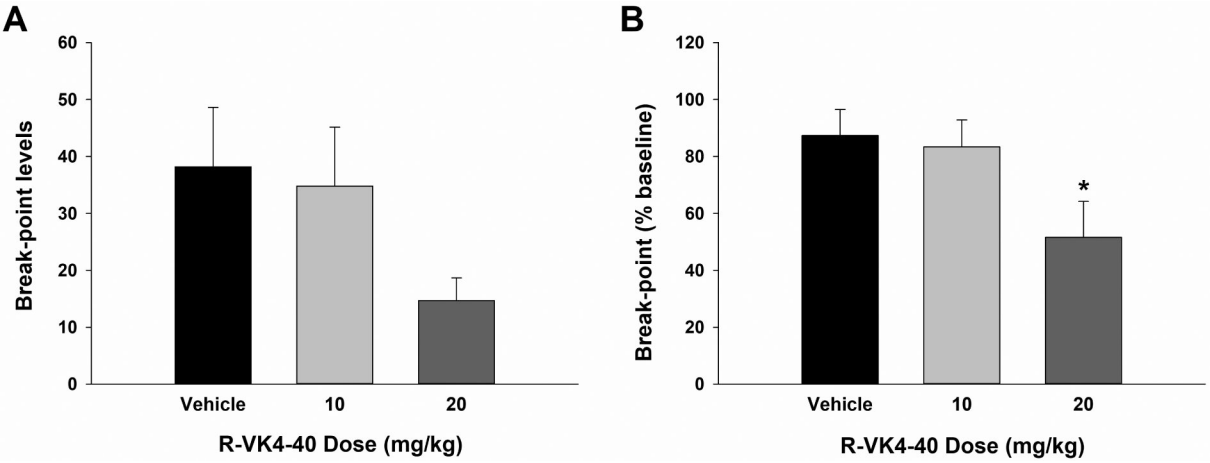

Figure 5.

Oxycodone self-administration under progressive-ratio (PR) reinforcement. ***A:*** Break-points for oxycodone self-administration in the presence or absence of *R*-VK4-40. ***B:*** Normalized break-points over baseline immediately before the testing day (% change in break-point). **p* < 0.05 compared to vehicle group.

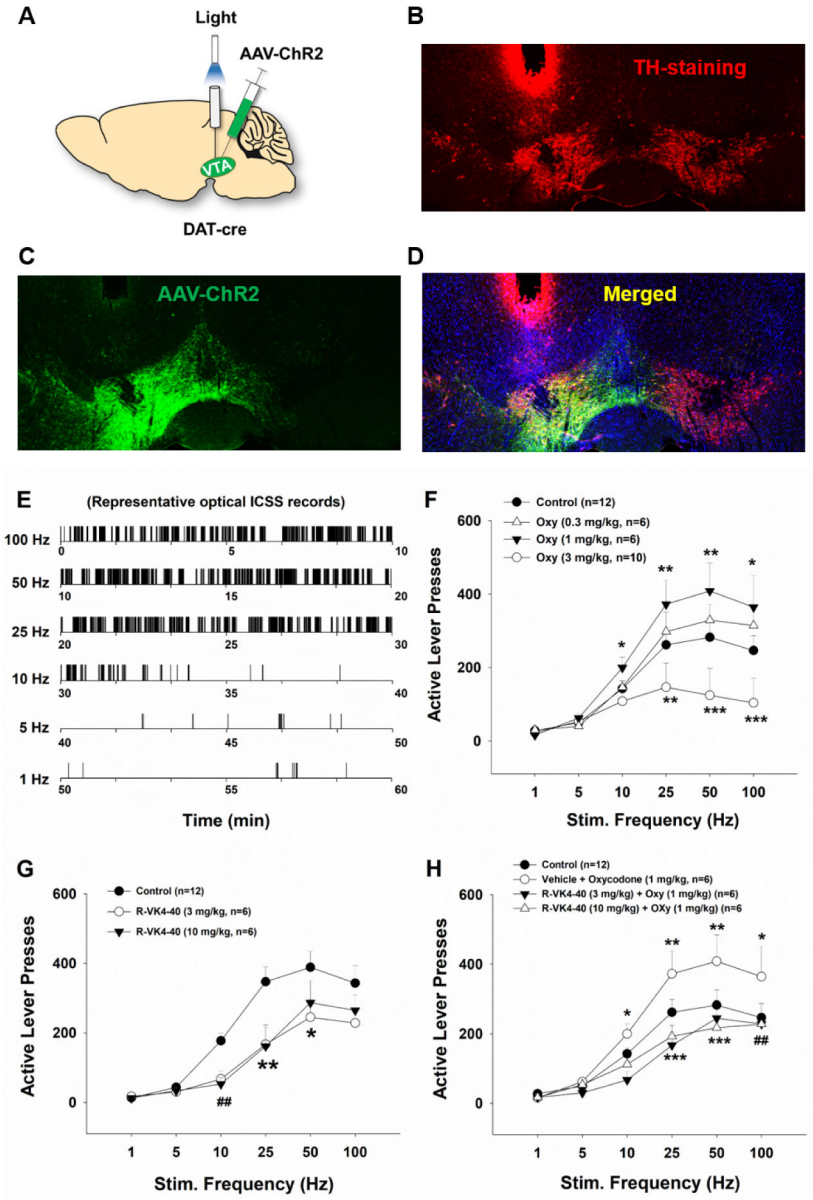

Figure 6.

Effects of *R*-VK4-40 and/or oxycodone on optical brain-stimulation reward in DAT-Cre mice. ***A***: Schematic diagrams illustrating the target brain region (VTA) of the AAV-DIO-ChR2-EGFP microinjections and intracranial optical fiber implantation (left). ***B, C, D***: Representative images of TH-immunostaining (red) and fluorescent ChR2-EGFP expression (green) in the VTA. ***E***: Representative rate-frequency curve under baseline conditions. ***F:*** Systemic administration of oxycodone produced dose-dependent biphasic effects – lower doses upward-shifted, while higher doses downward-shifted stimulation-response curves. ***G:*** Systemic administration of *R*-VK4-40 alone dose-dependently shifted the stimulation-response curve downward. ***H***: Pretreatment with *R*-VK4-40 dose-dependently blocked 1 mg/kg oxycodone-enhanced optical ICSS. *$p < 0.05$; **$p < 0.01$, ***$p < 0.001$ compared to the vehicle control group; $^{\#\#}p < 0.01$ (10 mg/kg *R*-VK4-40), compared to control groups.

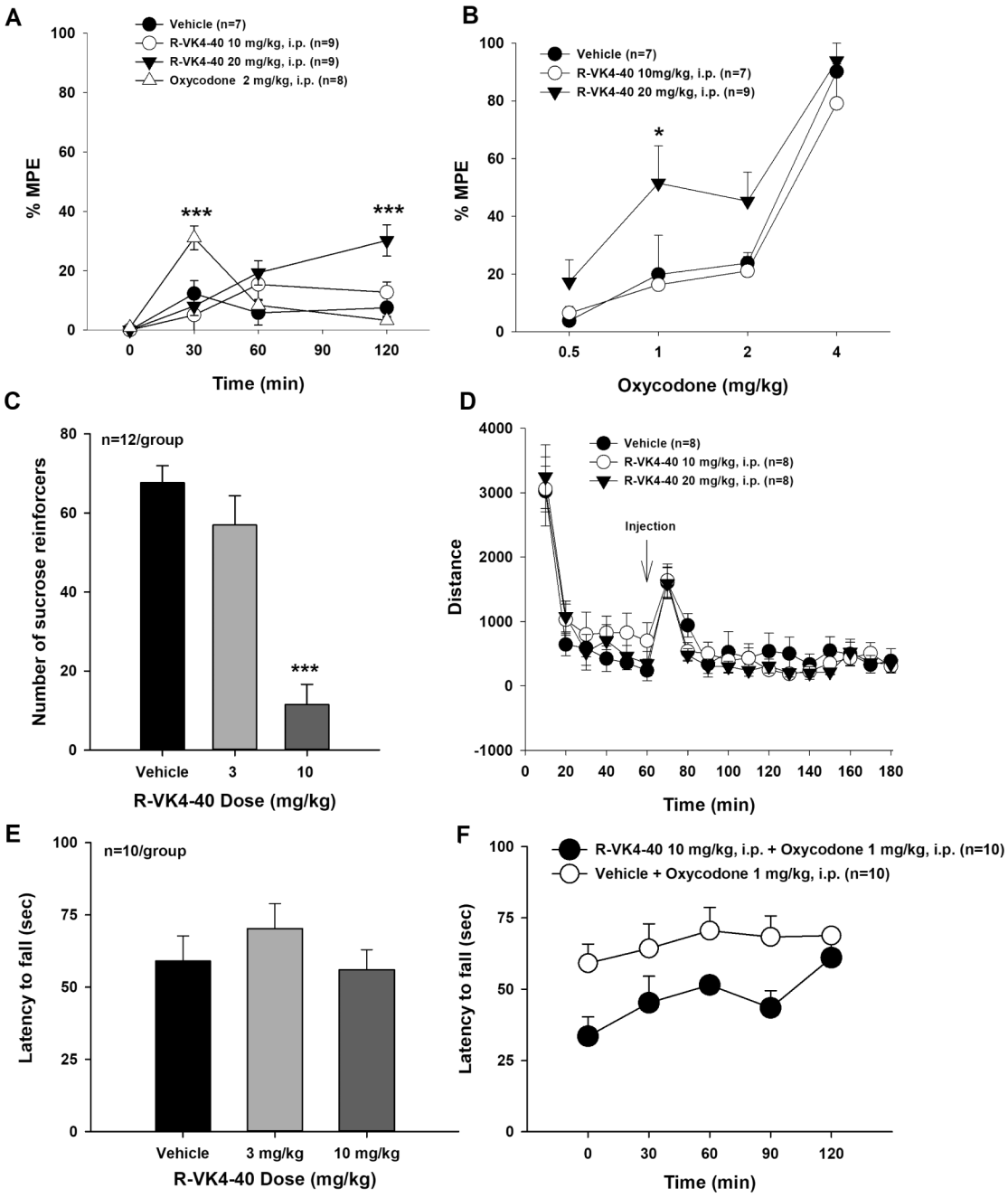

Figure 7:

Effects of *R*-VK4-40 and/or oxycodone on thermal nociceptive responses in rats. ***A*:** The time course of the analgesic effects of oxycodone or *R*-VK4-40 alone as assessed in the hotplate test. ***B***: Thirty-minute pretreatment with *R*-VK4-40 produced an upward shift in the dose-response curve of oxycodone-induced analgesia at 15 minutes post-injection, suggesting enhanced antinociceptive effects. **C**: Thirty-minute pretreatment with *R*-VK4-40 dose-dependently suppressed sucrose self-administration in mice. **D:** Open-field locomotor behavior indicating that *R*-VK4-40 had no effect on locomotion in rats. **E:** Rotarod mobility is similarly unaffected by *R*-VK4-40 treatment in mice. **F:** Combination of *R*-VK4-40 with

1 mg/kg oxycodone produced a non-significant trend towards locomotor sedation in mice. *p<0.05, ** p<0.01, ***p<0.001 compared to control groups.